

UKAEA-CCFE-CP(23)47

L. Howlett, I. Cziegler, S. Freethy, H. Meyer

L-H transitions and intermediate behaviours on MAST and MAST-U

This document is intended for publication in the open literature. It is made available on the understanding that it may not be further circulated and extracts or references may not be published prior to publication of the original when applicable, or without the consent of the UKAEA Publications Officer, Culham Science Centre, Building K1/O/83, Abingdon, Oxfordshire, OX14 3DB, UK.

Enquiries about copyright and reproduction should in the first instance be addressed to the UKAEA Publications Officer, Culham Science Centre, Building K1/O/83 Abingdon, Oxfordshire, OX14 3DB, UK. The United Kingdom Atomic Energy Authority is the copyright holder.

The contents of this document and all other UKAEA Preprints, Reports and Conference Papers are available to view online free at scientific-publications.ukaea.uk/

L-H transitions and intermediate behaviours on MAST and MAST-U

L. Howlett, I. Cziegler, S. Freethy, H. Meyer

L-H transitions and intermediate behaviours on MAST and MAST-U

L. Howlett^{1,2}, I. Cziegler¹, S. Freethy², H. Meyer²

¹ York Plasma Institute, School of PET, University of York, York, UK

² United Kingdom Atomic Energy Authority, Culham Centre for Fusion Energy, Abingdon, UK

Due to the increase in fusion power, H-mode is a favoured operating regime for future devices. For a tokamak shot to transition into H-mode, the net power must cross a threshold $P_{net} \geq P_{LH}$. The power threshold P_{LH} is important to know for future devices, as it will determine the size of the machine as well as the amount of external heating power necessary to obtain H-mode. Predicting P_{LH} is complicated by the lack of a comprehensive model and requires the use of empirical scaling laws. Existing scaling laws based on large multi-machine databases have come up with power law dependencies of several parameters, such as density n_e , magnetic field B_T and surface area S , but many more parameters which have been experimentally shown to influence P_{LH} in often complex ways are not yet captured. For low aspect ratio tokamaks specifically, the commonly used scaling laws such as the ITER scaling by Martin et al. [1] predict a P_{LH} much lower than the observed experimental values. P_{LH} follows a U-shaped n_e dependence [2, 3, 4], with a low-density [2] and a high-density branch, where fits and scalings are performed on the high- n_e branch. One of the effects which have been experimentally shown to influence P_{LH} but not yet quantified or included in scalings is the divertor configuration, such as the reduction of P_{LH} with a slot divertor on C-Mod [5] or with reduced X-point height on JET [6]. Understanding which of the many divertor parameters is responsible and the physics behind it motivates the study of the L-H transition in the new Super-X divertor on MAST-U.

MAST data from an L-H transition experiment has been analysed to find the density dependence of the power threshold. The net power vs density parameter space for double null shots with $I_p \approx 750$ kA on MAST has been mapped in a dedicated L-H transition experiment. All the shots were heated with NBI, and the net power is taken as $P_{net} = P_{nbi} + P_{ohm} - dW/dt$. The stored energy W is calculated with a high time resolution run of the equilibrium code EFIT. The ohmic power P_{ohm} was calculated with two different methods, using either EFIT or the transport code TRANSP, leading to slightly different results, so two results for the overall P_{net} were obtained, with the TRANSP version using the captured NBI power calculated by TRANSP for P_{nbi} and the EFIT version using the input power. The uncertainties in the P_{net} components (including from varying the choice of smoothing window for W) were combined to form the error bars on P_{net} . The radiated power is not generally included in P_{net} for these studies or for the scalings, but calculations for $P_{net} - P_{rad}$ were also compared, showing that aside from

the expected overall reduction in the values, the inclusion of P_{rad} does not change the results.

In general, time periods in a shot can be classified to be in L-mode, H-mode, or an intermediate/boundary case. Exploring these in more detail, with example traces shown in Fig. 1, the H-modes for most of the density range in this experiment are ELMy (with $f_{ELM} = 0.5 - 0.6$ kHz), and often preceded by one or more short i-phases [7], which are visible in D_α as regular oscillations of 3-4kHz. As the density is reduced, the pre-H i-phase becomes longer, and at lower densities still, the H-mode becomes

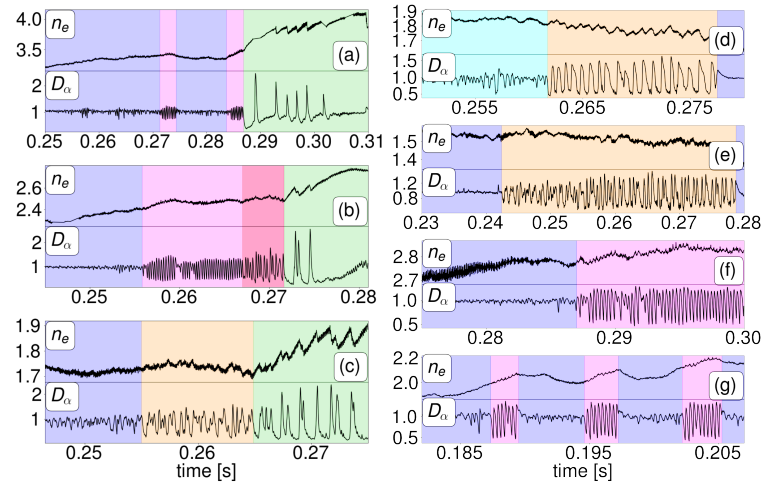


Figure 1: n_e [$10^{19}m^{-3}$] and D_α traces showcasing the categories used in the P_{LH} studies. Left: H-modes at different densities (decreasing from (a) to (c)), with (a) showing a typical H-mode, (b) a long pre-H i-phase and (c) a dithery H-mode. Boundary behaviours are shown on the right, with dithery periods in (d) and (e) and i-phases in (f) and (g).

dithery (appearing to move in and out of H-mode). If P_{net} at these low densities is close to P_{LH} but insufficient for H-mode, the plasma will exhibit similar dithery periods but with lower confinement and therefore less of a rise in n_e . A further boundary behaviour for P_{net} close to P_{LH} is the appearance of i-phases without a subsequent L-H transition. It should be noted that H-mode points were taken at the start of the pre-H i-phase, as the stored energy W begins to increase, a feature of H-mode confinement. Since the heating power could not be scanned during a shot at MAST, and the H-mode entry was controlled through keeping the plasma in an unfavourable-biased disconnected double null configuration until the desired conditions were achieved [8], the (n_e, P_{net}) combination for L-H transitions correspond to H-mode accessible values, not necessarily the actual P_{LH} , and the $P_{LH}(n_e)$ curve should be determined from the boundary between the H-mode-accessible and -inaccessible regions in the plots. The results for both methods (Fig. 2) show the characteristic U-shaped density dependence, with $n_{e,min} = 2 - 2.5 \times 10^{19} m^{-3}$, where the low-density branch is bordered by a large region of dithery and intermittent periods, and the boundary throughout the density range contains i-phases. The results are compared to the Martin scaling [1] which is expected to under-predict P_{LH} , as well as a modified scaling to accommodate low aspect ratio devices by Takizuka [9]. Though the Takizuka scaling is slightly improved, both scalings under-predict P_{LH} by an order of magnitude. Fitting a simple power

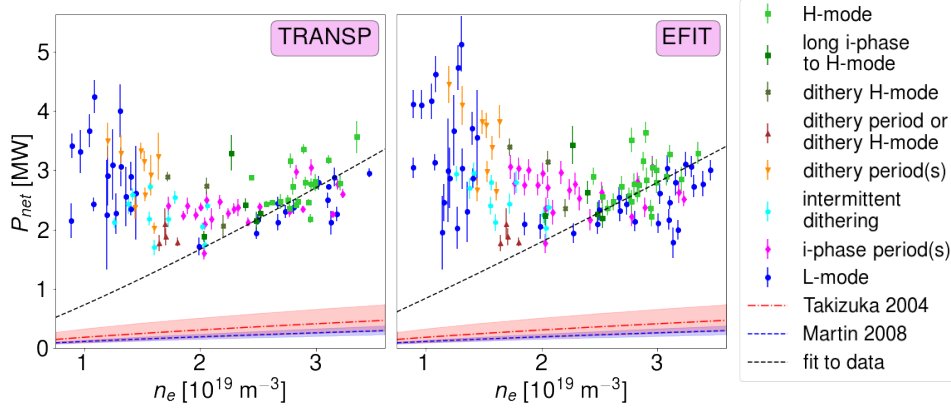


Figure 2: P_{net} vs n_e results for TRANSP and EFIT methods with the P_{LH} Martin and Takizuka scalings as well as a fit to the n_e dependence of the high- n_e branch of the data.

law for the density dependence to the high-density branch of the data returns

$$P_{LH} [MW] = 11.35 \times n_{e20}^{1.19} \quad P_{LH} [MW] = 10.41 \times n_{e20}^{1.09}$$

for the TRANSP and EFIT methods respectively. The density exponent is 50-66% higher than for the scalings ($\sim n_{e20}^{0.7}$), though not significant with the data scatter, but the majority of the discrepancy between the fit and the scalings is due to the leading factor, which is out by over an order of magnitude and includes both known non- n_e and unknown parameter dependencies. Due to the limited amount of data available the cause of the large discrepancy between scalings and the observed P_{LH} on MAST can not be determined at this time.

One of the physics features of the L-H transition is the development of a steep well in the radial electric field at the edge. The edge E_r is thought to mainly be determined by the gradient of the ion pressure, and the key role of the ion heat flux q_i in the edge has been shown on several devices. In these other studies [10, 11], q_i was shown to increase linearly with density, in contrast to the non-linear dependence of P_{LH} , suggesting the existence of a critical ion heat flux per particle. A lower q_i per input power at low densities (and low collisionalities), for example due to reduced ion-electron coupling, could present an explanation for the low-density branch of P_{LH} . The analysis to compare the edge q_i before the L-H transition at different densities, as well as compare general features of q_i and the electron heat flux q_e for this data set is ongoing.

To study the divertor geometry dependence of the L-H transition further, experiments have been performed on MAST-U comparing conventional (CD) and Super-X (SX) divertor performance. The results are preliminary and more experiments are scheduled for the next campaign. H-mode access was found to be easier in CD than both MAST-U SX and MAST CD plasmas, with frequent ohmic H-modes and stable L-mode scenarios more difficult to attain. A preliminary qualitative conclusion suggests a significantly higher P_{LH} for SX compared to CD.

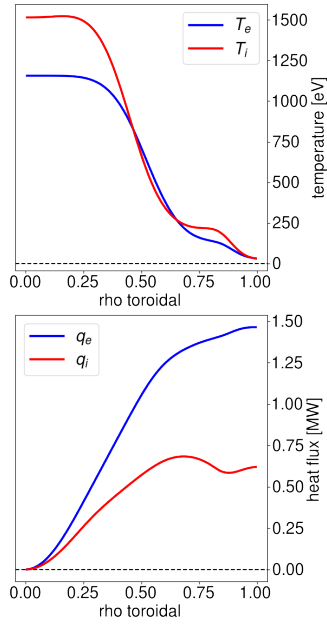


Figure 3: Ion and electron temperature and heat flux profiles at transition to a low- n_e H-mode.

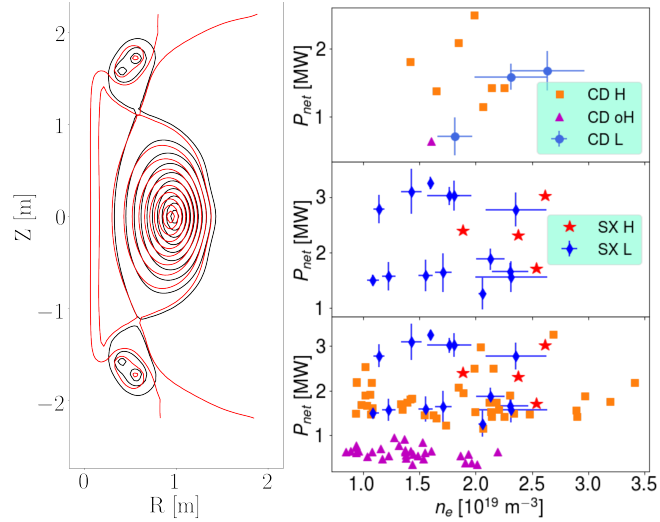


Figure 4: Left: Equilibria of conventional divertor (CD) in black and Super-X (SX) in red. Right: Preliminary results from a P_{LH} study in SX (middle), with a comparable CD study (top), and the large existence range of CD H-modes compared with the SX study (bottom). (oH = ohmic H-mode)

For our experiment, we performed a limited density and power scan in SX at 600kA, with four shots achieving an L-H transition during the established Super-X phase (Fig. 4). The strong detachment for the SX divertor as well as the appearance of early modes require further consideration for the analysis and future experiments. This study will be continued in the next campaign, with the beam emission spectroscopy diagnostic providing edge turbulence data during the transition which will be used to calculate the nonlinear energy transfer between turbulence and zonal flows, thought to be an important trigger of the L-H transition [12].

References

- [1] Y.R. Martin, T. Takizuka, Journal of Physics: Conference Series **123**, 012033 (2008)
- [2] P. Sauter et al., Nuclear Fusion **52**, 012001 (2012)
- [3] P. Gohil et al., Nuclear Fusion **51**, 103020 (2011)
- [4] Y. Ma et al., Nuclear Fusion **52**, 023010 (2012)
- [5] Y. Ma et al., Plasma Physics and Controlled Fusion **54**, 082002 (2012)
- [6] Y. Andrew et al., Plasma Physics and Controlled Fusion **46**, A87 (2004)
- [7] H. Zohm et al., Physical Review Letters **72**, 2 (1994)
- [8] H. Meyer et al., Plasma Physics and Controlled Fusion **50**, 015005 (2008)
- [9] T. Takizuka, Plasma Physics and Controlled Fusion **46**, A227 (2004)
- [10] F. Ryter et al., Nuclear Fusion **54**, 083003 (2014)
- [11] M. Schmidtmayr et al., Nuclear Fusion **58**, 056003 (2018)
- [12] I. Cziegler et al., Nuclear Fusion **55**, 083007 (2015)